

T.Ye. Korochkova¹, V.O. Mashira^{1,2}, T.Yu. Gromovoy¹, A.D. Terets^{1,3}

DIFFUSIVE TRANSPORT ALONG A STRUCTURED SURFACE: RATCHET EFFECT STABILITY WHEN CHANGING THE POTENTIAL PROFILE TYPE

¹ *Chuiiko Institute of Surface Chemistry of National Academy of Sciences of Ukraine
17 General Naumov Str., Kyiv, 03164, Ukraine, E-mail: tais.crust@gmail.com*

² *Frantsevich Institute for Problems of Materials Science of National Academy of Sciences of Ukraine
4 Krzhizhanovsky Str., Kyiv, 03142, Ukraine, E-mail: mashira.vasyl@gmail.com*

³ *Faculty of Physics, Taras Shevchenko National University of Kyiv*

4 Academician Glushkov Avenue, Kyiv, 03127, Ukraine, E-mail: terets.andrey@gmail.com

The phenomenon of the ratchet effect provides the motion a large number of molecular machines, existing in nature and artificially created nanomechanisms, capable to initiate directed diffusion movement along periodic structures. Two key factors, necessary for the ratchet effect occurrence, are the presence of asymmetry in the system and the organization of the non-equilibrium fluctuations process. Asymmetry can be created directly by the stationary potential form, in the field of which unidirectional motion is organized. Double-sine (smooth) and sawtooth (piecewise-linear) potential profile dependences are encountered most frequently when designing models. The source of such dependence can be a chain of collinearly located dipoles on the surface of a solid. The purpose of this work was to study the influence on the ratchet effect of changing the model potential class from smooth to piecewise linear. For this purpose, two methods of approximation of the double sinusoidal potential by a sawtooth were considered. The first, simple, consists in connecting the extremum points with straight-line segments, preserving the height of the potential barrier and the coordinates of the extrema. The second, the least squares method (LSM), reproduces the slopes of the smooth potential as closely as possible. A model of a stochastic Brownian motor with small fluctuations of the potential energy by a harmonic signal was chosen for the comparative analysis. This model has no limitations in the ranges of the environment temperature and fluctuation frequency parameters, so the ratchet effect can be studied in all operation modes of the motor. It is shown that at sufficiently high temperatures for any asymmetry of potentials, approximation by the simple method gives better results, and at high frequencies – the LSM method. An algorithm for determining the best approximation method in the ranges of parameters that generate the largest flux values is proposed. It has been shown that for single-well double-sine potentials the approximate LSM-potential gives identical results of temperature-frequency dependences. Contour graphs of relative flux values were plotted, demonstrating parameters regions of the greatest identity (stability) of the ratchet effect and the region of the greatest difference.

Keywords: *dipole chain, orientation-structured system on a surface, controlled diffusion transport, near-surface mass transfer, Brownian motors, ratchet effect, potential fluctuations*

INTRODUCTION

Today, the task of modeling, designing and developing scientific theories of nanomechanism motion is relevant and promising in many fields of scientific research [1–4]. Nanoscale devices, regardless of their structure and functions, are immersed in a liquid or gaseous medium and experience thermal motion of molecules of the environment. The interaction between the particles and the medium is quite comparable in magnitude to other interactions acting on the nanodevice. The presence of such an interaction fundamentally distinguishes nanoscale motors from macroscopic devices [1]. Brownian motors

are a class of nanoscale mechanisms that use the thermal noise of the environment as one of the useful (necessary) components in generating their own motion [2]. The mechanism of Brownian motor operation is based on the idea of rectification the already existing chaotic Brownian motion of a nanoparticle with the help of spatial asymmetry created in the motor's surroundings and the unbiased fluctuations imposing into the system. These fluctuations, on the one hand, are a source of energy (“fuel”) for the motor and, at the same time, a factor that disrupts the thermodynamic equilibrium state, due to which the occurrence of directional motion (occurrence of the ratchet effect)

becomes possible [1–4]. The mechanism of Brownian motor operation explains the motion of many naturally occurring molecular devices that carry out intracellular transport (for example, the motion of kinesin and dynein along microtubules [6, 7]), perform complex collective processes in living organisms (for example, myosin and actin, which are responsible for muscle contraction) [2, 3, 8], as well as less obvious processes related to the generation of motion: proton ATP synthase, the implementation of active membrane transport through ion channels, rotation of molecular rotors, *etc.* [5–9]. In addition to biological ones, there are many artificially created nano-mechanisms built on the phenomenon of the ratchet effect: particles moving in a liquid or gaseous solutions in the field of action of a periodic asymmetric potential [10, 11], the motion of electrons in semiconductors [12], devices for particle separation [13–15], transport of nano-cargoes similar to protein motors along periodic fibers [16–18], manipulation of charged membrane components, proteins and lipids, in a structured lipid bilayer [19, 20], creation of various molecular rotors near surfaces [21–24] *etc.*

In Chuiko Institute of Surface Chemistry of the National Academy of Sciences of Ukraine since 2003, fundamental research in the field of Brownian motor theory and its application to mass transfer processes near the surface of a solid body is carried out. Thus, a number of models were proposed demonstrating the ratchet effect occurrence near the surface. It was analytically proven that Brownian particles that cyclically gain and lose electric charge (on-off model [1]) can move unidirectionally along ordered dipole chains on the surface of a solid [25, 26]. It was shown that charged particles will move unidirectionally under the action of an externally applied alternating electric field, which with a certain frequency brings the particle closer and further away from the surface and changes its potential energy [27]. It was theoretically investigated that resonant laser irradiation of a particle with a variable dipole moment initiates the directional motion of this particle in a spatially periodic potential (the concept of a photomotor). It was analytically demonstrated that the sorbed polar molecule in the potential of hindered rotation moves around unidirectionally under the action of an

alternating electric field (molecular rotor model) [27], *etc.*

So, the ratchet effect is the mechanism by which the Brownian motor works, as it initiates a directed, not a chaotic, motion. Two key factors necessary for the ratchet effect occurrence are the presence of asymmetry in the system and the organization of the process of non-equilibrium fluctuations. If the asymmetry is created directly by the shape of the stationary potential profile, then we are talking about such systems as ratchets [1], and then the properties of the surface will be decisive in the generation of fluxes. By manipulating the composition and structure of the surface, we can create such a potential profile that will generate a flux of nanoparticles of a given magnitude and direction. The presence of a structured substrate, which is a source of spatial periodicity and asymmetry, provides the possibility of implementing at least two concepts of Brownian motors near the surface: initiating the directed diffusion motion of Brownian particles along the structured chains of adsorbed molecules of the surface layer [25, 26] or the unidirectional rotation of an adsorbed polar molecule, which is in the field of action of the potential of neighboring atoms [26, 27]. That is, combining the theory of Brownian motors with surface physics and chemistry is a promising interdisciplinary direction that allows constructing models of non-biological nanodevices, which, in turn, can be used to create controlled diffusion transport in near-surface layers or in various studies of surface properties by molecular rotors [26, 27].

In general, model potential profiles, in the field of which directed diffusion motion is generated, are divided into two large classes: smooth and piecewise linear (that is, those that contain areas of large gradients of potential energy change). These classes are headed by two “archetypal” potential profiles [2], the most characteristic and most often used – double-sine [2, 28] and sawtooth [2, 3] dependences. Many well-known models have been formulated and calculated for them, and analytical solutions in various approximations have been found [1–4]. Despite the fact that these potentials are both single-well, asymmetric and visually similar in shape, the resulting ratchet effect can differ significantly in its properties, such as, for example, the possibility of temperature-

frequency control of the motion direction [29]. In addition, since the sawtooth potential is much easier to parameterize and often analytical solutions are easier to obtain precisely for it, it may be necessary to replace the model potential [25, 26] from smooth to sawtooth within the framework of one model to obtain an analytical solution. Peculiarities of the ratchet effect depending on the potential profile shape were studied only within the framework of particular approximations (for example, comparative studies of high-frequency different classes ratches [30, 31]). However, when designing artificial Brownian motors operating in certain frequency and temperature regimes (for example, devices for particle separation [1–5]), in order to select a specific periodic substrate, knowledge about the influence of the stationary potential profile shape on the resulting flux over the entire range of control parameters is required. So, the purpose of this work was to study the influence on the ratchet effect of changing the model potential class from smooth to piecewise linear. The approximation of small fluctuations is best suited for this task, because it is based on a “leading” stationary potential, the shape of which changes weakly during fluctuations. If the perturbing factor is chosen to be the same as the other control parameters of the system, it is possible to directly highlight the influence of the shape of our model “master potential” on the magnitude and direction of the resulting flux, which is intended to be done in this work. Also, in order to formulate recommendations for obtaining the most similar ratchet effect when replacing potentials within the framework of one problem, it is advisable to consider different types of approximation and their results in the full ranges of control parameters, which will allow to identify areas of parameters that ensure the identity and maximum divergence of the generated fluxes, as well as clarifying the physical factors of such behavior.

In the next section, a description of the motion dynamics of a Brownian particle in an alternating potential will be considered and a numerical procedure for calculating the main characteristics of the ratchet effect in the approximation of small fluctuations will be given. Then the potential of a dipole chain as a component of a structured surface will be reviewed, and options for selecting a simple model potential will be discussed. After that, the

methods of approximating smooth potentials by sawtooth potentials will be described, the obtained calculation results depending on various model parameters will be considered and analyzed, and conclusions will be formulated.

RATCHET EFFECT CALCULATION IN THE FRAME OF SMALL FLUCTUATION APPROXIMATION

Typically, the ratchet effect is described by considering the one-dimensional motion of a Brownian particle in an external force field characterized by a potential energy $U(x, t)$ that depends on the coordinate x and time t . Dynamics of studied particle-motor is described by the Smoluchowski equation for the distribution functions $\rho(x, t)$, defining the location of the particle in a time moment t [3, 29, 32–34]:

$$\frac{\partial}{\partial t} \rho(x, t) + \frac{\partial}{\partial x} J(x, t) = 0, \quad (1)$$

$$J(x, t) = -De^{-\beta U(x, t)} \frac{\partial}{\partial x} e^{\beta U(x, t)} \rho(x, t). \quad (2)$$

Equation (2) sets the probability flux $J(x, t)$, $D \equiv (\beta\zeta)^{-1}$ – the diffusion coefficient and ζ – the friction coefficient.

The approximation of small potential energy fluctuations, developed by the team of authors [32], is used, first of all, to describe a wide class of artificially created molecular machines. It assumes that the potential profile $U(x, t)$ has an additive-multiplicative form [34, 35]:

$$U(x, t) = u(x) + \sigma(t)w(x), \quad (3)$$

in which the first term $u(x)$ describes the stationary (undisturbed) profile, and the second term $\sigma(t)w(x)$ describes the fluctuating component (disturbance). Small fluctuations of the potential energy correspond to the case when $w(x) \ll u(x)$. At the same time, it is assumed that $|\sigma(t)w(x)| / k_B T \ll 1$, and the ratio $|u(x)| / k_B T$ is considered arbitrary.

We will use a harmonic signal $w(x)$ with amplitude w , spatial period of the system L and phase shift λ_0 as a small fluctuating component of the potential $U(x, t)$ [34, 35], that is easy to realize experimentally for non-biological ratchets [36, 37]:

$$w(x) = w \cos[2\pi(x/L - \lambda_0)]. \quad (4)$$

The function $\sigma(t)$ is responsible for the time dependence of the potential energy $U(x, t)$. Most often, fluctuations are introduced into the system by stochastic dichotomous process, i.e. one that reflects the course of random homogeneous phenomena characterized by average values. Stochastic (random) fluctuations are typical for protein motors: due to the cyclic course of the chemical reaction of ATP hydrolysis, conformational changes occur in the motor protein, which causes fluctuations in the effective potential profile [3, 6, 7, 11], or for artificial nanomechanisms in which a random number generator or the course of chemical reactions is used to switch states [38].

Let us assume that a symmetrical dichotomous process is implemented in our system, in which $\sigma(t)$ takes two values $+1$ or -1 and alternating with a given frequency of transitions γ . That is, with this type of fluctuations, the motor particle has potential energy (3) in the form $U(x, t) = u(x) \pm w(x)$, and switching between two states ($u(x) + w(x)$) and ($u(x) - w(x)$) occurs randomly with an average frequency γ .

The approximation of small fluctuations [34] makes it possible to develop a numerical procedure for finding the main characteristic of the Brownian motor - the constant flux of particles $J \equiv \langle J(x, t) \rangle$, using the Green's function method [34, 35]. For this purpose, all periodic components of the potential energy $u(x)$, $w(x)$ and functions of the equilibrium distributions in the stationary potential $u(x)$ $\rho^{(0)}(x) = e^{-\beta u(x)} / \int_0^L dx e^{-\beta u(x)}$ and $q(x) = e^{\beta u(x)} / \int_0^L dx e^{\beta u(x)}$ are represented in the form of Fourier series ($f(x) = \sum_p f_p e^{ik_p x}$ (where $k_p = 2\pi p / L$, $p = 0, \pm 1, \pm 2, \dots$; $f(x)$ - each of these functions), and the procedure consists in inverting the matrix, and finding Green's function Fourier components of the $S_{pp'}$ and further double summation to find the flux value J [29]:

$$J = -i(\pi\beta Dw)^2 \sum_{pp'} k_p S_{pp'} [q_{-p+1} Z_{p'}^{(+)} + q_{-p-1} Z_{p'}^{(-)}],$$

$$Z_{p'}^{(\pm)} = e^{\pm 4\pi i \lambda_0} \rho_{p' \pm 1}^{(0)} - \rho_{p' \mp 1}^{(0)},$$

$$\sum_{\bar{p}} [(Dk_p^2 + \Gamma)\delta_{p\bar{p}} + \beta Dk_p k_{p-\bar{p}} u_{p-\bar{p}}] S_{\bar{p}p'} = -\frac{1}{L} \delta_{pp'},$$

(5)

where $\Gamma = 2\gamma$. The desired velocity of the Brownian motor will be equal to $\langle v \rangle = LJ$.

We note that the described procedure does not specify the form $u(x)$ of the stationary potential, but only the perturbing component (4). In the subsequent sections of the article, based on system (5), numerical calculations of the flux will be carried out to juxtapose the contributions of the two stationary profiles that we are comparing.

THE POTENTIAL OF A DIPOLE CHAIN

It is known that an orientationally structured system of adsorbed polar molecules can form on the surface of a solid under certain conditions: the ground state of two-dimensional dipole systems corresponds to ferroelectric or antiferroelectric structures (dependent on the type of two-dimensional lattice of the adsorbate), consisting of chains with collinear orientations of dipole moments along the chain axis [25]. Such a dipole chain with a period L creates an electrostatic field (Fig. 1), in which a charged particle q has a potential energy $V_z(x, z)$, which can be written in the following form [25]:

$$V_z(x, z) = V_0 \sum_{h=1}^{\infty} h K_0 \left(\frac{2\pi h}{L} z \right) \sin \left(\frac{2\pi h}{L} x \right),$$

$$V_0 = \frac{2q\mu}{\epsilon_0 L^2},$$

(6)

where μ is the dipole moment of the adsorbed molecule, ϵ_0 is the electric constant, and $K_0(x)$ is the Macdonald function. The dependence of the potential energy on the spatial coordinates (6) is obviously periodic along the axis with a period L (like a dipole chain) and rapidly decreases with distance from the chain: the amplitude's value decreases to 0 when the ratio z/L tends to 1 [25]. In addition to the amplitude, periodic dependences are characterized by an asymmetry parameter - the ratio of the distance between adjacent extrema to the spatial period, and if this parameter differs from 0.5, then it is an asymmetric dependence [3, 25]. For the potential energy $V_z(x, z)$, the asymmetry parameter also changes (decreases) when moving away from the chain and goes to 0.5 as the ratio z/L tends to 1 [25].

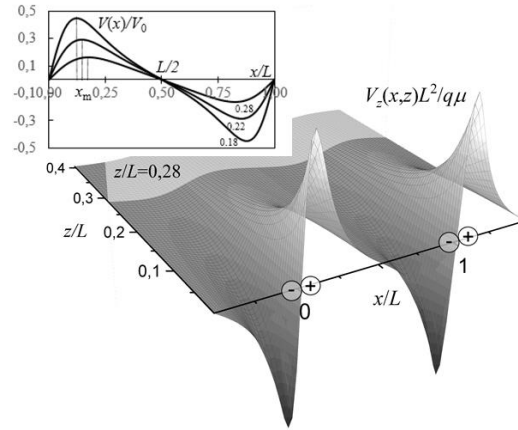


Fig. 1. Spatial dependence of the potential energy of a charged particle q near the dipole chain, and (in the upper left tab) its dependence $V(x)$ for fixed values z/L (labeled on the curves). During calculations, series (6) was limited to $h = 20$

If the external alternating electric field for some time has only a tangential component that keeps the particle-motor at a certain fixed distance z/L from the chain, then for this period the parameters of the potential energy are constant, and it will depend only on the coordinate x : $V(x) = V_z(x, z_{const})$. The tab of Fig. 1 shows the dependences of the potential energy $V(x)/V_0$ for three fixed values of the ratio $z/L = 0.18, 0.22, 0.28$. That is, the shape of the potential energy spatial dependence of the interaction between the charged particle-motor and the dipole chain, as an example of a real system, will significantly depend on the distance to the chain at which the motion will occur. Thus, in work [25] a fixed value $z/L = 0.28$ was chosen (the curve with the smallest amplitude in the tab of Fig. 1), and for it the approximation by a double-sine dependence (restriction of the series (6) to two terms) is quite sufficient:

$$v(x) = u_0 \left[\sin(2\pi x/L) + \frac{1}{4} \sin(4\pi x/L) \right],$$

$$u_0 = \frac{2q\mu}{\varepsilon_0 L^2} K_0(1.76). \quad (7)$$

The double-sine potential first appeared in the theory of Brownian engines in this form [28], and is now encountered most often [3]. But when approaching the dipole chain with increasing amplitude and asymmetry, it is obvious that function (7) will no longer approximate the dependence $V(x)$, and even if it remains in the class of smooth potentials, the coefficient at the second harmonic must be variable. For small

z/L ones (see the curve with the largest amplitude in the tab of Fig. 1), it is obvious that approximation by a saw-like function will be more successful. In the next section, using the example of a double-sine dependence with variable coefficients, options for its approximation by a sawtooth dependence will be considered.

METHODS OF APPROXIMATION OF A DOUBLE-SINE POTENTIAL BY A SAWTOOTH

Setting the double-sine potential. The potential energy of a particle in the form of a double-sine potential (or biharmonic potential) is generally given by the formula:

$$u_{\sin}(x) = A_1 \sin(2\pi x/L) + A_2 \sin(4\pi x/L), \quad (8)$$

that is, it represents the sum of two sinusoids of different periods L and $L/2$ with independent amplitudes, respectively, A_1 and A_2 having the dimension of energy. If we enter the dimensionless coefficient $\alpha = A_2/A_1$, then the function (8) will take the form:

$$u_{\sin}(x) = A_1 \left[\sin(2\pi x/L) + \alpha \sin(4\pi x/L) \right]. \quad (9)$$

The double-sine potential is an antisymmetric periodic function with a period L , which has centers of symmetry at the zero points of the function $Ln/2$, $n \in \mathbb{Z}$ (see Fig. 2 a), is single-well at $\alpha < 0.5$ and double-well at $\alpha > 0.5$. This function is spatially asymmetric, and its coefficient of asymmetry is usually determined by the ratio of the distance between the nearest

minimum and maximum to the spatial period by analogy with the sawtooth potential [3]:

$$\kappa_h = (x_{\max} - x_{\min}) / L. \quad (10)$$

The use of the potential in form (8) or (9) is convenient in the case $\alpha < 1$ that, i.e., the contribution of the second harmonic with a half period is small, and it practically does not increase the amplitude of the potential. For sufficiently large values, it is more convenient to use the potential with additional normalization, which allows one to separate the asymmetry of the potential and its amplitude and make them independent parameters [29]:

$$\begin{aligned} \tilde{u}_{\sin}(x) &= u_0 f(x), \\ f(x) &= C_n(\alpha) [\sin(2\pi x / L) + \alpha \sin(4\pi x / L)], \end{aligned} \quad (11)$$

where the coefficient $C_n(\alpha)$ is calculated by the formulas:

$$\begin{aligned} C_n(\alpha) &= [2(\sin(2\pi x_{\max} / L) + \alpha \sin(4\pi x_{\max} / L))]^{-1}, \\ x_{\max} &= \arccos[(2\sqrt{8 + (4\alpha^2)^{-1}} - \alpha^{-1}) / 8] / 2\pi. \end{aligned} \quad (12)$$

The normalization coefficient is calculated for each value α and is equal to doubled value of the expression of formula (10) in square brackets at the maximum point x_{\max} (see Fig. 2 a). That is, for any value α , the dimensionless expression $f(x)$ has a full unit amplitude.

Setting the sawtooth potential. The sawtooth potential is a periodic piecewise linear function, for its specification the spatial period is divided

into several (two or three) intervals, on which the equations of straight lines are specified. Most often, the sawtooth potential is given by two segments in the following form [26]:

$$u_s(x) = u \begin{cases} x/l, & 0 < x < l, \\ (L-x)/(L-l), & l < x < L, \end{cases} \quad (13)$$

with this definition $u_s > 0$, it is periodic ($u_s(x + nL) = u_s(x)$, $n \in Z$) and does not belong to the classes of symmetric or antisymmetric functions. The characteristics of the potential are very easy to determine: the amplitude (energy characteristic) is equal to the coefficient u , and the coefficient of asymmetry is equal to $\kappa_s = l / L$.

In tasks for which it is necessary to carry out an approximation by a sawtooth potential, it is more convenient to specify it in the form of an antisymmetric function (see Fig. 2 a, large-dashed dependence):

$$\tilde{u}_s(x) = v_0 \begin{cases} x/x_0, & 0 < x < x_0, \\ (L/2 - x)/(L/2 - x_0), & x_0 < x < L/2. \end{cases} \quad (14)$$

With this method of setting, the function $\tilde{u}_s(x)$ can take both positive and negative values; x_0 – maximum coordinate, v_0 – potential amplitude. It is obvious that dependences (13) and (14) correspond to one and the same function shifted along the axis x by x_0 , and along the energy axis by v_0 , that is $l = 2x_0$, $u = 2v_0$, and $\kappa_s = 2x_0/L$.

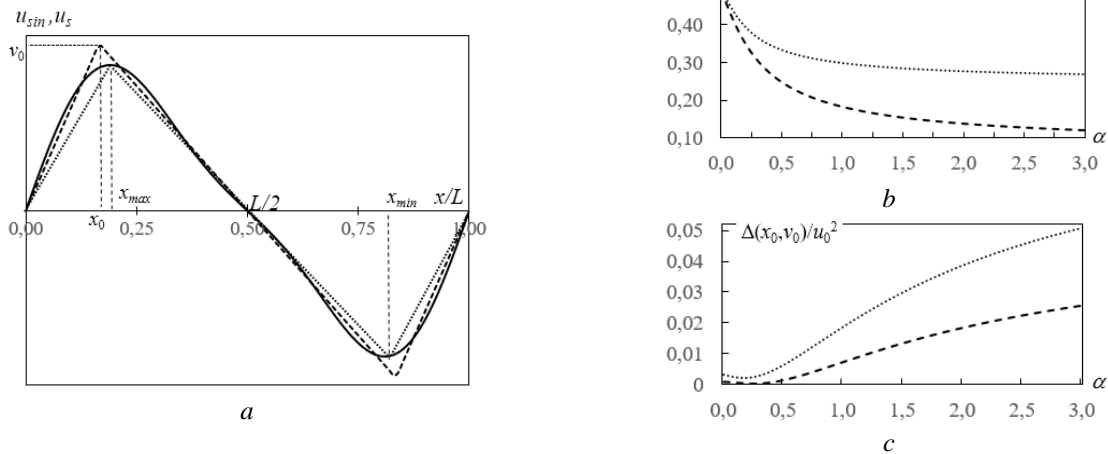


Fig. 2. a – the potential of a double-sine (11) (solid line) and its variants of approximation by a sawtooth potential; dependences of b – the asymmetry coefficients and c – the value of the quadratic deviations (15) on the parameter α for the simple approximation method (dotted lines) and the LSM method (dashed lines)

Since only the derivative of the potential energy is included in the Smolukhovsky equation, the position of the potential function along the energy axis is not important. A certain problem is the shift along the axis, which affects the phase shift between the stationary and fluctuating components of the potential, so it must be taken into account in the calculations accordingly.

Methods of approximation. Usually, works (see, for example, [25, 26]) use a simple method of transition between defined potentials, which is the connection of maxima and minima of the double-sine potential with segments (see Fig. 2 *a*, dotted lines). A sawtooth potential is formed, in which all characteristics completely match with the characteristics of the double-sine potential: the coordinates of the extrema $x_0 = x_{\max}$ and the asymmetry coefficient $\kappa_s = \kappa_h$. If we approximate the potential given by expression (9), then the resulting amplitude will be equal to A_1 , if we use additional normalization and the original dependence (11), then the amplitude of the approximation potential will be equal to u_0 .

Another approximation option is the least squares method (LSM), which was discussed in detail in our article [35]. It consists in finding the minimum of the integral factor of quadratic deviations between the double-sine potential and the sawtooth dependence function in the entry (14):

$$\Delta(x_0, v_0) = \int_0^{x_0} dx \left[\tilde{u}_{\sin}(x) - \frac{v_0}{x_0} x \right]^2 + \int_{x_0}^{L/2} dx \left[\tilde{u}_{\sin}(x) - \frac{v_0}{L/2 - x_0} (L/2 - x) \right]^2, \quad (15)$$

which allows numerical methods to obtain the values and coordinates of the maximum x_0 and v_0 . According to the LSM method, the parameters of the sawtooth potential are calculated in such a way that the “distances” between the functions at each point are minimal, and the forms of dependence are maximally similar, as a result, we obtain a potential with a different position of the maximum, amplitude and, accordingly, the asymmetry parameter (Fig. 2 *a* and 2 *b*, dashed lines).

Table 1 shows the parameters of sawtooth potentials formed by two types of approximation, simple and LSM, calculated for some fixed values

of the parameter α : the position of the maximum x_{\max} and the asymmetry coefficient κ_h for the simple method (which match with the characteristics of the double-sine potential); and LSM approximation parameters: the position of the maximum x_0 , the asymmetry coefficient κ_h and the amplitude’s ratio of the double-sine and approximating potentials v_0 / A_1 for the case of the initial dependence in the form (9) and v_0 / u_0 – in the form (11).

Table 1 shows the data corresponding to parameter values α from 1/8 to 3, but since the double-sine potential remains single-well only when $\alpha < 0.5$ the applicability of the approximation for large values α is under the question. In addition, the total quadratic deviations have the smallest values in the range $0 < \alpha < 0.5$ (see Fig. 2 *c*), and with further α growth steadily increase, which indicates an increasingly large discrepancy between the original and approximation function. In this regard, we carried out most of the calculations for the range of $\alpha < 1$.

It is worth adding that the considered types of approximation will be suitable and similarly implemented for any smooth potential: a simple method will consist in connecting the largest potential barrier and the deepest well with segments, and the LSM method will consist in solving the resulting system of equations when searching for the minimum value of expression (15) when replacing the potential $\tilde{u}_{\sin}(x)$ with another investigated.

CALCULATION RESULTS

For a comparative analysis, the numerical procedure (5) was applied consistently to three stationary potentials: a double-sine with a normalization coefficient (11), and two approximate saw-tooth potentials (14) with different parameters obtained by the simple and LSM methods. The corresponding Fourier components are given by the following expressions:

$$\tilde{u}_{\sin p} = \frac{u_0 C_n(\alpha)}{2} [\mp i \delta_{p,\pm 1} \mp i \alpha \delta_{p,\pm 1}], \quad (16)$$

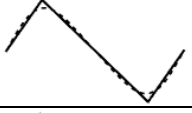

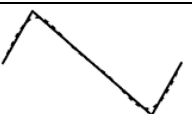

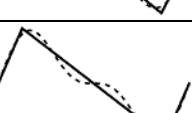
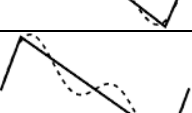
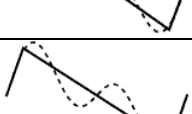
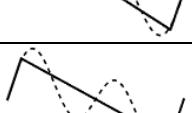
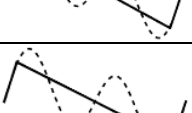
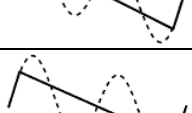
$$\tilde{u}_{\text{simple } p} = u_0 \frac{e^{-2\pi i \kappa_h p} - 1}{4\pi^2 p^2 \kappa_h (1 - \kappa_h)}, \quad (17)$$

$$\tilde{u}_{\text{LSM } p} = v_0 \frac{e^{-2\pi i \kappa_s p} - 1}{4\pi^2 p^2 \kappa_s (1 - \kappa_s)}, \quad (18)$$

and the Fourier components of the fluctuation function $w(x)$ have the form:

$$w_p = \frac{W}{2} \left[e^{2\pi i \lambda_0} \delta_{p,-1} + e^{-2\pi i \lambda_0} \delta_{p,1} \right]. \quad (19)$$

Table 1. The most used values of the parameter α and the corresponding characteristics of the sawtooth potential for two types of approximation

α	$C_n(\alpha)$	Simple method			LSM method			Form of potential profiles
		x_{\max}	κ_h	x_0	κ_s	v_0 / A_1	v_0 / u_0	
1/8	0.486	0.234	0.468	0.201	0.402	1.228	1.193	
1/6	0.476	0.208	0.416	0.188	0.375	1.236	1.178	
1/4	0.454	0.190	0.380	0.166	0.331	1.258	1.143	
1/3	0.430	0.180	0.360	0.149	0.297	1.286	1.107	
1/2	0.385	0.166	0.332	0.126	0.251	1.349	1.038	
3/4	0.328	0.155	0.310	0.105	0.209	1.456	0.955	
1	0.284	0.149	0.298	0.092	0.184	1.569	0.892	
1.5	0.223	0.142	0.284	0.078	0.155	1.806	0.805	
2	0.183	0.138	0.276	0.070	0.139	2.048	0.748	
3	0.134	0.134	0.268	0.061	0.122	2.537	0.681	

In addition to the parameter α corresponding to the shape and asymmetry of the potential profiles, and the phase shift between the stationary and fluctuating components λ_0 , the model system in which the ratchet effect is

observed is characterized by the following external parameters: the temperature of the environment, which we introduce as a dimensionless parameter βu_0 – the ratio of the potential barrier’s height to thermal energy, and

the frequency of potential fluctuations γ is a dimensionless parameter $\gamma L^2 / D$ (L^2 / D – nanoparticle diffusion time over the distance of the spatial period) [26]. The influence of the parameter λ_0 was studied in detail in [29]: it determines the cyclic dependence of the magnitude and sign of the flux, which is the same for two types of potentials, so its variation is outside the scope of this study. However, even excluding λ_0 , it still remains to investigate the dependence of the flux J on three parameters (α , βu_0 , $\gamma L^2 / D$), which, with simultaneous imaging, involves the construction of a four-dimensional surface. For a detailed analysis of the results, consider a series of cross-sectional drawings with different combinations of fixed parameters.

When analyzing the results, the behavior of the ratchet effect depending on two parameters – temperature and frequency – is of primary interest. Fig. 3 shows the surfaces of flux values J calculated for the double-sine potential with $\alpha = 1/4$ with the corresponding potential approximated by the LSM method. Both surfaces show a non-monotonic dependence on both parameters (which is typical for ratchets [1–4, 26]), and the location of the maxima of the surfaces is close, but with a certain shift. The essential difference lies in the amplitude of the effect: the sawtooth stationary component gives a much larger flux in the region of the maximum (Fig. 3 b).

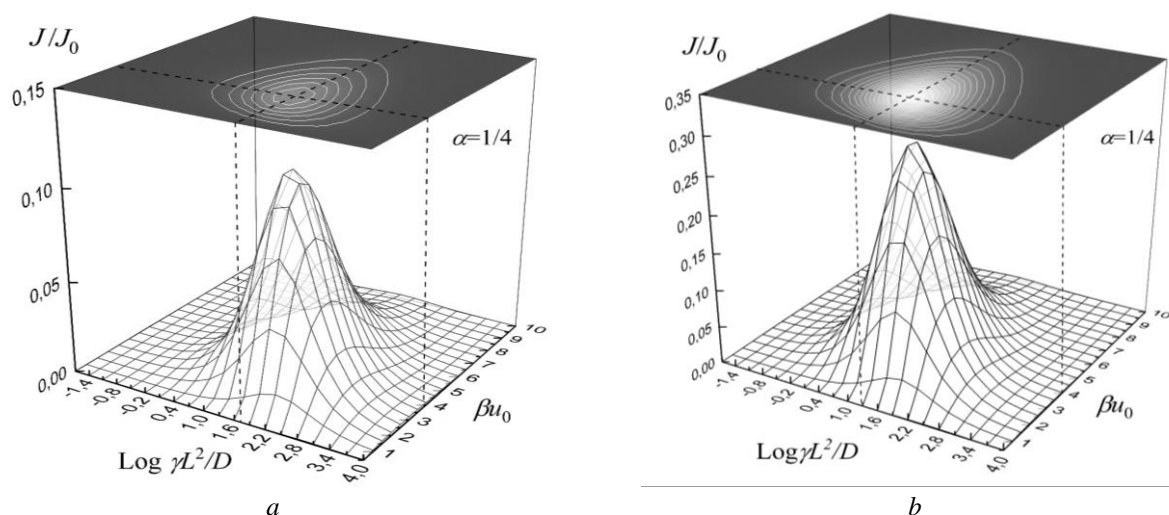


Fig. 3. The nanoparticle flux values J surface in units $J_0 = (\beta D w^2) / (u_0 L^2)$ depending on temperature βu_0 and frequency $\gamma L^2 / D$ parameters in the model with stationary double-sine (a) and approximated sawtooth potential by the LSM method (b). Calculations were carried out with a fixed value of $\alpha = 1/4$ and phase shift $\lambda_0 = 0.25$

In the next three figures, we will study the behavior of the flux J depending on various model parameters for the entire set of studied forms of the potential energies. The solid lines correspond to the values of the flux calculated for the double-sine dependence, the dotted lines to the approximation by the simple method, and the dashed lines – by the LSM method.

Fig. 4 shows the dependence of the flux value in units $J_0 = (\beta D w^2) / (u_0 L^2)$ on dimensionless parameters βu_0 and $\gamma L^2 / D$ in pairs for three values of the parameter α : $1/8$ and $1/4$ (corresponding to the single-well type of a double-sine potential) and $3/4$ (double-well potential). Temperature dependences (left

column of the graphs) are plotted at fixed $\gamma L^2 / D = 50$, and frequency dependences (right column) at fixed $\beta u_0 = 2$ (gray curves) and $\beta u_0 = 6$ (black curves).

All shown figures, in fact, represent sections of surfaces of flux values in variables (βu_0 , $\gamma L^2 / D$), similar to those shown in Fig. 3, planes parallel to the axes. In the central regions of the graphs of temperature dependences in Fig. 4 a, c, e of the flux values, corresponding to the simple and LSM methods, compete with each other, so it is impossible to determine the most appropriate approximation method. Nevertheless, it can be found out for a fixed value of βu_0 , based on its position relative to the

maximum of the flux dependence curve on the temperature parameter: deviating from the maximum into the high-temperature region (left side of the graph), the fluxes closest in value are given by the simple method, and when moving to the right from a certain value of βu_0 , different for different α , the LSM method shows a better correspondence. Depending on the frequency parameter (the three right graphs of Fig. 4 *b, d, f*), the location of the curves for different methods almost does not change, so the temperature dependence is sufficient to determine the optimal approximation method. The fact is also important that in the high-frequency region (right wing of Fig. 4 *b, d, f*) for all α values, the LSM approximation method shows better correspondence.

The study of the influence of the factor α that determines the shape and asymmetry of the potentials is presented in Fig. 5, consisting of a graphs series calculated for different values βu_0 from 0.1 to 10 (Fig. 5 *a-d*) and the same frequency of $\gamma L^2 / D = 50$. As the parameter α increases, the asymmetry coefficients of the potentials decrease, which leads to an increase in the flux values: monotonically for a sawtooth potential (provided the amplitude is the same) [26] and non-monotonically for a double-sine [29]. This tendency persists for solid and dotted dependences. When the parameter α for the flux created by the LSM method increases (dashed lines), the increase in asymmetry is compensated by the decrease in amplitude, which gives a behavior similar to the behavior of the flux for double-sine.

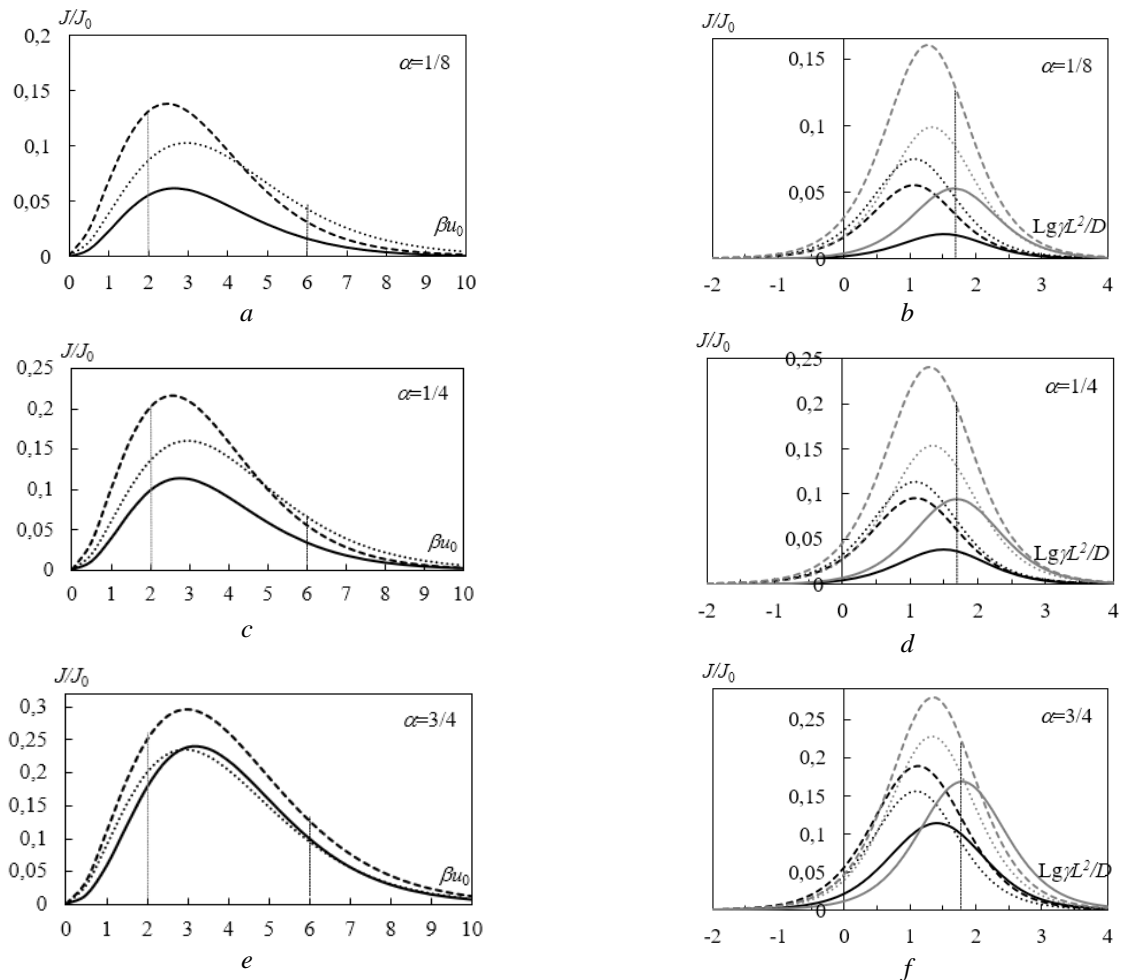


Fig. 4. Calculated temperature and frequency dependences of the flux J / J_0 for three values of the parameter α (shown in the graphs). Graphs *a, c, e* are plotted with fixed $\gamma L^2 / D = 50$ ($Lg[\gamma L^2 / D] = 1.70$), and *b, d, f* – with fixed $\beta u_0 = 2$ (gray curves) and $\beta u_0 = 6$ (black curves). Corresponding values on the axes of temperature and frequency parameters are marked with dashed lines. Calculations were performed with a fixed value and phase shift $\lambda_0 = 0.25$

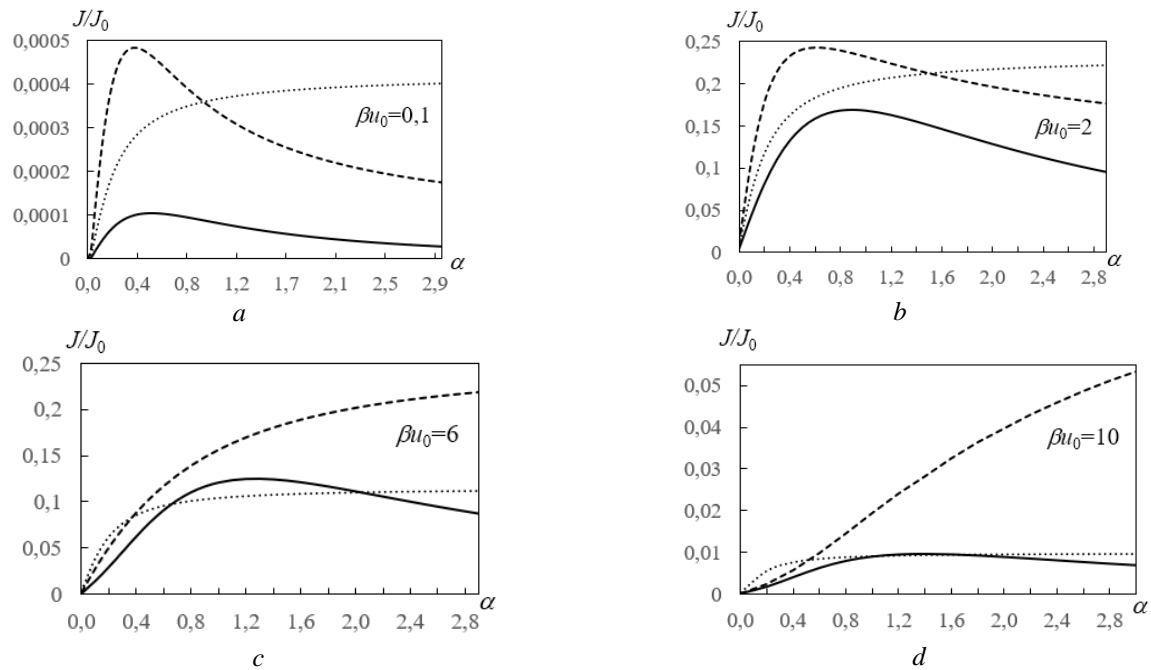


Fig. 5. Dependences of the flux J / J_0 on the parameter α for various fixed values βu_0 (shown in the graphs) at a fixed values of $\gamma L^2 / D = 50$ and $\lambda_0 = 0.25$

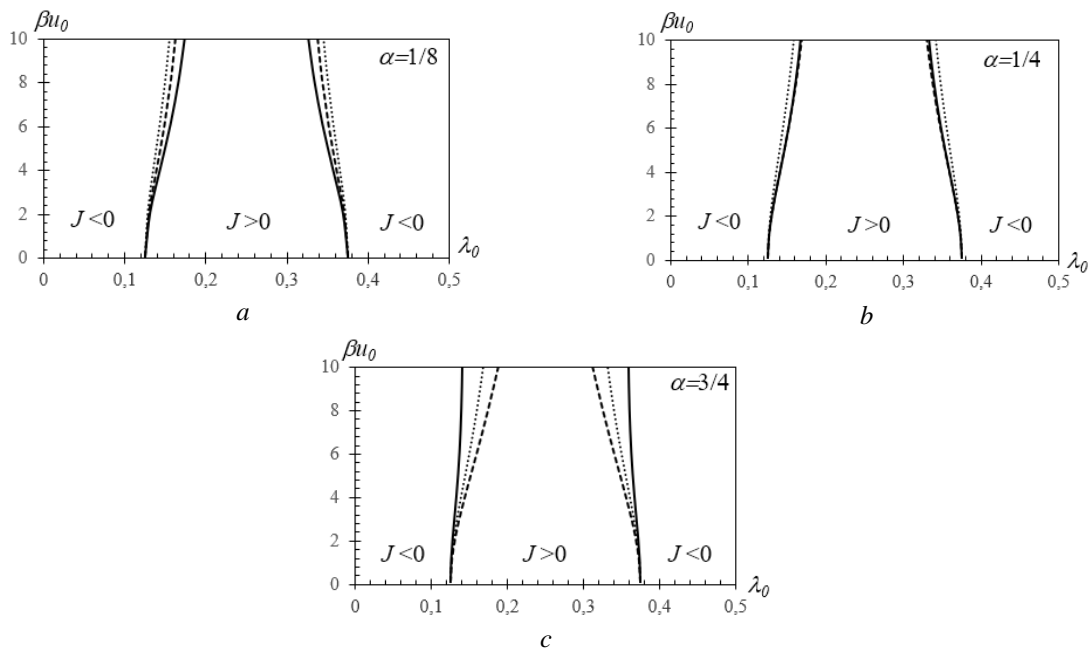


Fig. 6. Diagrams of the motor stopping points location relative to the parameters βu_0 and λ_0 for three parameter values $\alpha : 1/8, 1/4$ and $3/4$ (a, b, c , respectively). All dependences are built at a fixed value $\gamma L^2 / D = 0.1$

Fig. 6 shows diagrams of motor stopping points depending on the variables βu_0 and λ_0 . They determine the ratio of these parameters, which ensure the occurrence of a ratchet effect in a certain direction (that is, a flux of a certain sign). Previous studies [29] showed that low-frequency regions are the most sensitive to

temperature-frequency control, so the value $\gamma L^2 / D = 0.1$ was chosen for comparative analysis. For the cases of values $\alpha : 1/8, 1/4$, the stopping points curves are very close (especially with the dependence calculated by the LSM method), i.e., the regions of sign constancy are, in fact, identical, and for the values $\alpha < 0.5$

corresponding to the single-well potential, the temperature-frequency dependence direction of the velocity of the motor with a double-sine potential and a sawtooth potential constructed by the LSM method are identical. For the case $\alpha < 3/4$ (Fig. 6 c), the differences in the regions of sign constancy are significant, i.e., in the region of low temperatures (the region of large values of βu_0) for controlling fluxes generated by different types of potentials, it will be different, and the use of approximation potentials is inappropriate.

For the most frequently used form of the double-sine potential with $\alpha = 1/4$, we have carried out an additional level comparative analysis of the fluxes created by the double-sine J_{sin} and the sawtooth J_{saw} (constructed by the LSM method) potentials. Fig. 7 a shows the contour graph of the flux ratio J_{saw}/J_{sin} , and Fig. 7 b – values of the relative deviation of fluxes:

$$\Delta_J = (J_{sin} - J_{saw}) / J_{sin} . \quad (20)$$

from the parameters βu_0 and $\gamma L^2 / D$. The darker areas of the graph in Fig. 7 a correspond to the areas of the parameters for which the differences in the ratchet effect will be maximal, and the darker areas in Fig. 7 b is the closest value of the fluxes. The greatest coincidence is characterized by the range of large values of the frequency parameter $\gamma L^2 / D \in (10^{2.5}, 10^4)$ and high and medium temperatures, for which it is possible to find such a value of the temperature parameter βu_0 that the difference between the fluxes does not exceed 0.05. The biggest difference is in the areas of medium temperatures and low frequencies $\gamma L^2 / D < 10^{-0.2}$, for which the ratio reaches a value of J_{saw}/J_{sin} 6 or more.

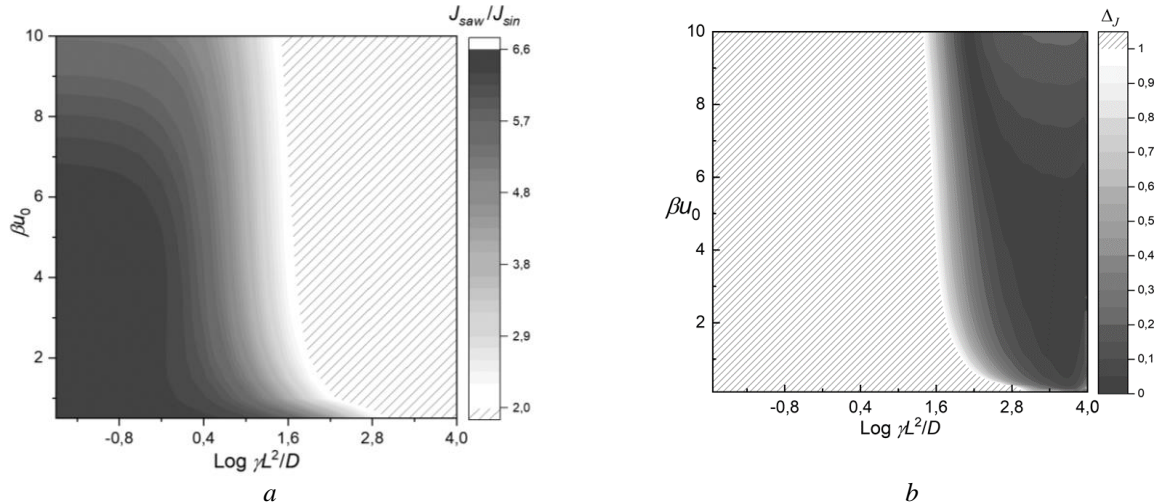


Fig. 7. a – areas of difference of the ratchet effect: contour graph of the ratio J_{saw}/J_{sin} for a range of values $J_{saw}/J_{sin} > 2$; b – regions of the identity of the ratchet effect: values of the relative deviation of fluxes Δ_J for the range of values of $\Delta_J < 1$. Regions $J_{saw}/J_{sin} < 2$ in Fig. a – $\Delta_J > 1$ and in Fig. b marked with dashes. Calculations were carried out with a fixed value of parameters $\alpha = 1/4$ and phase shift $\lambda_0 = 0.25$

DISCUSSION AND CONCLUSIONS

The phenomenon of the ratchet effect is diverse and widespread [1–5], but there are literally several mechanisms behind it. To isolate them, describe them theoretically, model, be able to predict, modify, learn to control them, and, finally, artificially reproduce them – these are the tasks and goals of the theory of Brownian motors. In addition to considering individual models, the theory of Brownian motors is aimed at finding and identifying the general properties of the ratchet effect as an object of its study.

The most widely used in the theory of Brownian motors are double-sine (smooth) and sawtooth (piecewise-linear) dependences of potential energy. The source of such periodic asymmetric electrostatic potential can be a chain of collinearly located dipoles. Tasks of the research was to find how the ratchet effect will behave when the class of the model potential is changed from smooth to piecewise linear, and to choose the optimal approximation method for different ranges of model parameters, which would minimize changes in the resulting flux.

To compare the ratchet effects created by these two types of stationary potentials, a model of a stochastic Brownian motor with small potential energy fluctuations the by a harmonic signal, which has no limitations in the ranges of the medium temperature and the frequency of fluctuations, was chosen. In this case, the ratchet effect can be studied in all modes of operation of the motor, and the obtained result can be used in various narrower approximations.

To accomplish the task, two approximation methods of double-sine potential by sawtooth were considered - the simple (by means of which the extremum points are connected by segments) and the least squares method (LSM). In general, any two asymmetric single-well potentials with similar asymmetry can be considered close dependences, which, after calculations using the same procedure, should give a very close result. However, for the theory of Brownian motors, their differences under certain conditions can be fundamentally important. A simple approximation method keeps the height of potential barrier and the position of the barrier and the well, i.e., if the ratchet effect is “started up” precisely by the barrier value and its location relative to the potential well on the spatial period, then this method should give a similar behavior of the flux magnitude. The LSM method repeats the shape and slopes as closely as possible (in fact, the sawtooth potential segments model conventional straight-line sections of double-sine potential), and if the ratchet effect is “launched” throughout the spatial period, this method will show a greater similarity of results. In addition, different modes of operation may have their own peculiarities.

To visualize general view of the patterns from external parameters – temperature βu_0 and frequency $\gamma L^2 / D$, flux values surfaces generated by the double-sine potential with a fixed $\alpha = 1/4$ and corresponding sawtooth potential constructed by the LSM method were plotted. They demonstrated the same nature of the dependences – non-monotonic, with a similar position of the maximum and a significantly larger amplitude for the sawtooth potential (see Fig. 3). The next series of two-dimensional graphs of sequentially depicted temperature and frequency dependences of the flux J (Fig. 4) showed that in the region of average values of temperature and frequency it is impossible to indicate the optimal approximation method due

to the difference in the position of the maxima and the resulting competition of values. But, for fixed external parameters, it is sufficient to obtain the temperature dependence to determine the approximation method. However, in the boundary regions, the behavior of the fluxes turned out to be more stable: at high temperatures for any values of α , the simple method gives the best results, and at high frequencies – the LSM method. A family of graphs of the behavior of fluxes as a function of the parameter α (Fig. 5) for different temperatures shows that in the high-temperature approximation, in principle, replacing the potential class greatly distorts the result, and in the region of average temperatures for single-well double sine potentials, the simple method is preferable, and with a further decrease temperature ($\beta u_0 > 4$), greater correspondence will be shown by the LSM method. A conclusion that is important for practical use in calculations follows from the diagrams of motor stopping points with different stationary potentials (Fig. 6): for single-well double sine potentials (Fig. 6 *a, b*), the LSM approximation method gives identical dependences, that is, for modeling temperature-frequency control, it makes no difference what type of potential to use; it is important to relate them to each other according to the LSM method. And, finally, as a result of an additional study of the areas of identity and difference flux values generated by the double-sine potential with a fixed and corresponding sawtooth potential constructed by the LSM method, the corresponding contour graphs of flux ratios were constructed. The performed calculations showed that identical values of fluxes are characteristic for the entire range of temperatures and high frequencies of potential fluctuations, and the biggest differences appear at low frequencies of fluctuations and especially for the average values of the temperature parameter of the environment. Physically, this can be explained by the fact that with a rapid change of the potential energy form, the particle “does not have time” to feel the “details” of this form, it reacts to the asymmetry “as a whole”, therefore the values of the velocities are almost the same in the two potential profiles. With slow fluctuations (in the adiabatic regime), on the contrary, the form of potential barriers and wells “come to the fore”: sharp extrema (casp points) of the sawtooth

dependence create a much greater “locking effect”, and the velocity from sawtooth potential is generated by 6 or more times higher than double-sine. The low-temperature region is characterized by a long stay of particles in the potential wells due to difficult thermal activation overcoming the barriers, the generated fluxes are small, and the influence of the potential shape on the motion characteristics is also reduced.

The works of other authors [30, 31, 38] previously concluded that the high-frequency limit of motor operation is the most sensitive to the shape of the potentials, while we received opposite results about identical flux values in this region. However, this contradiction can be explained by the difference in the formulation of the problems: indeed, the high-frequency region is sensitive to slopes, therefore the LSM method (which preserves slopes) does not distort the resulting flux, while the simple method in this region makes a big difference.

Thus, we performed a large-scale comparative study of the dependence of the behavior of the ratchet effect on the shape of the stationary potential profile. First of all, it is important for carrying out and optimizing future calculations of the diffusion transport characteristics along periodic structures of various types. Secondly, the results obtained made it possible to clarify and expand the previously known conclusions about high-frequency nanotransport and demonstrate the areas of parameters that are most sensitive to the class of model potential (smooth and containing cusp points). Finally, this work shows that ratchet effects created by related dependences (i.e. almost identical conditions) can differ in magnitude by several times, which can be used in the construction of highly efficient models of nanomechanisms.

Дифузійний транспорт вздовж структурованої поверхні: стійкість ретчет-ефекту при заміні типу потенціального профілю

Т.Є. Корочкова, В.О. Машира, Т.Ю. Громовий, А.Д. Терець

*Інститут хімії поверхні ім. О.О. Чуйка Національної академії наук України
вул. Генерала Наумова, 17, Київ, 03164, Україна, tais.crust@gmail.com*

*Інститут проблем матеріалознавства ім. І.М. Францевича Національної академії наук України
вул. Кржижановського, 3, Київ, 03142, Україна*

*Фізичний факультет, Київський національний університет імені Тараса Шевченка
просп. Академіка Глушкова, 4, Київ, 03127, Україна*

Явище ретчет-ефекту забезпечує рух багатьох існуючих в природі молекулярних машин та штучно створюваних наномеханізмів, що здатні ініціювати направлений дифузійний рух вздовж періодичних структур. Два ключові фактори, необхідні для виникнення ретчет-ефекту, – це наявність асиметрії в системі та організація процесу нерівноважних флуктуацій. Асиметрія може створюватись безпосередньо формою стаціонарного потенціалу, в полі дії якого організовано однонаправлений рух. Найчастіше зустрічаються подвійна синусоїдальна (плавна) і пилоподібна (кусково-лінійна) залежності потенціального профілю. Джерелом такої залежності може бути ланцюжок колінеарно розташованих диполів на поверхні твердого тіла. Задачею дослідження було знайти, яким чином зміниться ретчет-ефект при заміні класу модельного потенціалу з плавного на кусково-лінійний. Для цього було розглянуто два методи апроксимації подвійного синусоїдального потенціалу пилоподібним: простий (simple), при якому точки екстремумів з'єднуються прямолінійними сегментами та зберігається висота потенціального бар'єра і координати екстремумів, та метод найменших квадратів (LSM), що максимально близько моделює нахили плавного потенціалу. Для проведення порівняльного аналізу була обрана модель стохастичного броунівського мотора з малими збуреннями потенціальної енергії гармонійним сигналом, яка не має обмежень в діапазонах температури середовища та частоти флуктуацій, і ретчет-ефект можна досліджувати в усіх режимах роботи мотора. Показано, що за досить високих температур для будь-якої асиметрії потенціалів апроксимація методом simple дає кращі результати, а за високих частот – метод LSM. Запропоновано алгоритм визначення кращого методу апроксимації в областях параметрів, що генерують найбільші значення потоків. Встановлено, що для одноямних подвійних синусоїдальних потенціалів апроксимаційний LSM-потенціал дає ідентичні результати температурно-частотних

залежностей. Побудовано контурні графіки відносних величин потоків, що демонструють області параметрів найбільшого співпадіння (стабільності) ретчет-ефекту та області найбільшої розбіжності.

Ключові слова: дипольний ланцюжок, орієнтаційно-структурована система на поверхні, керований дифузійний транспорт, приповерхнєве масоперенесення, броунівські мотори, ретчет-ефект, флуктуації потенціалу

REFERENCES

1. Fornes J.A. *Principles of Brownian and Molecular Motors*. V. 21. (Springer Nature: Springer Series in Biophysics, 2021).
2. Hänggi P., Marchesoni F. Artificial Brownian motors: Controlling transport on the nanoscale. *Rev. Mod. Phys.* 2009. **81**: 387.
3. Reimann P. Brownian Motors: Noisy Transport far from Equilibrium. *Phys. Rep.* 2002. **361**(2–4): 57.
4. Cubero D., Renzoni F. *Brownian Ratchets: From Statistical Physics to Bio and Nano-motors*. (Cambridge University Press., 2016).
5. Credi A., Balzani V. *Molecular machines*. (1088press, Italy, 2020).
6. Okada Y., Hirokawa N. A Processive Single-Headed Motor: Kinesin Superfamily Protein KIF1A. *Science*. 1999. **283**(5405): 1152.
7. Howard J. *Mechanics of Motor Proteins and the Cytoskeleton*. Part II. (Sinauer Associates, Sunderland, Massachusetts, 2001).
8. Finer J.T., Simmons R.M., Spudich J.A. Single myosin molecule mechanics – piconewton forces and nanometre steps. *Nature*. 1994. **368**(6467): 113.
9. Gorre-Talini L., Spatz J. P., Silberzan P. Dielectroscopic ratchets. *Chaos*. 1998. **8**: 650.
10. Rousselet J., Salome L., Ajdari A. Directional motion of brownian particles induced by a periodic asymmetric potential. *Nature*. 1994. **370**(6489): 446.
11. Lipowsky R., Klumpp S. ‘Life is Motion’ – Multiscale Motility of Molecular Motor. *Physica A*. 2005. **352**(1): 53.
12. Kedem O., Lau B., Weiss E.A. Mechanisms of Symmetry Breaking in a Multidimensional Flashing Particle Ratchet. *ACS Nano Letters*. 2017. **11**(7): 7148.
13. Astumian D., Hänggi P. Brownian Motors. *Phys. Today*. 2002. **55**(11): 33.
14. Pamme N. Continuous flux separations in microfluidic devices. *Lab. Chip*. 2007. **7**(12): 1644.
15. Savel’ev S., Misko V., Marchesoni F., Nori F. Separating particles according to their physical properties: Transverse drift of underdamped and overdamped interacting particles diffusing through two-dimensional ratchets. *Phys. Rev. B*. 2005. **71**: 214303.
16. Lund K., Manzo A.J., Dabby N., Michelotti N., Johnson-Buck A., Nangreave J., Taylor S., Pei R., Stojanovic M.N., Walter N.G., Winfree E., Yan H. Molecular robots guided by prescriptive landscapes. *Nature*. 2010. **465**: 206.
17. Wickham S.F.J., Endo M., Katsuda Y., Hidaka K., Bath J., Sugiyama H., Turberfield A.J. Direct observation of stepwise motion of a synthetic molecular transporter. *Nat. Nanotechnol.* 2011. **6**: 166.
18. Cha T.G., Pan J., Chen H., Salgado J., Li X., Mao Ch., Choi J.H. A synthetic DNA motor that transports nanoparticles along carbon nanotubes. *Nat. Nanotechnol.* 2013. **9**(1): 39.
19. Krogh A., Larsson B., von Heijne G., Sonnhammer E. Predicting transmembrane protein topology with a hidden Markov model. Application to complete genomes. *J. Mol. Biol.* 2001. **305**(3): 567.
20. Overington J.P., Al-Lazikani B., Hopkins A.L. How many drug targets are there? *Nat. Rev. Drug Discovery*. 2006. **5**: 993.
21. Jiang X., O’Brien Z.J., Yang S., Lai L.H., Buenaflor J., Tan C., Khan S., Houk K.N., Garcia-Garibay M.A. Crystal fluidity reflected by fast rotational motion at the core, branches, and peripheral aromatic groups of a dendrimeric molecular rotor. *J. Am. Chem. Soc.* 2016. **138**(13): 4650.
22. Lien Ch., Seck Ch.M., Lin Y.-W., Nguyen J.H.V., Tabor D.A., Odom B.C. Broadband optical cooling of molecular rotors from room temperature to the ground state. *Nat. Commun.* 2014. **5**: 4783.
23. Cherioux F., Galangau O., Palmino F., Repenne G. Controlled directional motions of molecular vehicles, rotors, and motors: from metallic to silicon surfaces, a strategy to operate at higher temperatures. *Chem. Phys. Chem.* 2016. **17**(12): 1742.
24. Khodorkovsky Y., Steinitz U., Hartmann J.-M., Averbukh I.Sh. Collisional dynamics in a gas of molecular superrotors. *Nat. Commun.* 2015. **6**: 7791.
25. Korochkova T.Ye., Rozenbaum V.M. Drift of a Brownian particle due to the orientational structuring of the adsorbate. *Reports of the National Academy of Sciences of Ukraine*. 2004. **8**: 93. [in Russian].

26. Rosenbaum V.M. *Brownian motion and surface diffusion*. In: Physics and chemistry of the surface. Book 1. Physics of the surface (in two volumes). V. 2 (Part VI, Chapter 23). (Kyiv: Institute of Surface Chemistry. A.A. Chuiko National Academy of Sciences of Ukraine, Ltd. Interservis, 2015). [in Russian].
27. Tsyomik O.Y., Chernova A.A., Rozenbaum V.M. Near-surface Brownian motors governed by an alternating electric field. *Reports of the National Academy of Sciences of Ukraine*. 2009. **12**: 83. [in Russian].
28. Bartussek R., Hänggi P., Kissner J.G. Periodically rocked thermal ratchets. *Europhys. Lett.* 1994. **28**(7): 459.
29. Korochkova T.Ye. Pulsating brownian motor with smooth modeling potentials in the framework of small fluctuation approximation. *Him. Fiz. Tehnol. Poverhni*. 2024. **15**(2): 159. [in Ukrainian].
30. Doering C.R., Dontcheva L.A., Klosek M.M. Constructive role of noise: Fast fluctuation asymptotics of transport in stochastic ratchets. *Chaos*. 1998. **8**(3): 643.
31. Reimann P. *Stochastic Processes in Physics, Chemistry, and Biology*. (Berlin: Springer-Verlag, 2000).
32. Vysotskaya U.A., Shapochkina I.V., Korochkova T.Ye., Rozenbaum V.M. Stochastic Brownian motors with small potential energy fluctuations. *Chemistry, Physics and Technology of Surface*. 2017. **8**(3): 299. [in Russian].
33. Risken H. *The Fokker-Plank Equation. Methods of Solution and Applications*. (Springer, Berlin, 1984).
34. Gardiner C.W. *Handbook of stochastic Methods for physics, chemistry and the Natural sciences*. 2nd edition, (Springer-Verlag Berlin, 1985).
35. Korochkova T.Ye. Piecewise-linear approximation of the potential relief of a brownian motors. *Surface*. 2017. **9**(24): 3. [in Russian].
36. Roth J.S., Zhang Y., Bao P., Cheetham M.R., Han X., Evans S.D. Optimization of Brownian ratchets for the manipulation of charged components within supported lipid bilayers. *Appl. Phys. Lett.* 2015. **106**(18): 183703.
37. Lau B., Kedem O., Schwabacher J., Kwasnieskiab D., Weiss E.A. An introduction to ratchets in chemistry and biology. *Mater. Horiz.* 2017. **4**(3): 310.
38. Schadschneider A., Chowdhury D., Nishinari K. *Stochastic Transport in Complex Systems: From Molecules to Vehicles*. 1st Edition. (Amsterdam: Elsevier Science, 2010).

Received 11.08.2024, accepted 05.03.2025